JOURNAL OF Materials CHEMISTRY

Synthesis and transport properties of substituted $Tl_2Mn_2O_7$ pyrochlore

W. Cheihk-Rouhou,[a] P. Strobel,[a] C. Chaillout,[a] S. M. Loureiro,[a] R. Senis,[b] B. Martinez,[b] X. Obradors[b] and J. Pierre[c]

[a]*Laboratoire de Cristallographie CNRS, BP166, 38042 Grenoble Cedex 9, France. E-mail: strobel@labs.polycnrs-gre.fr*
[b]*Instituto de Ciencia de Materiales de Barcelona, CSIC, Bellaterra 08193, Spain*
[c]*Laboratoire Louis Néel, CNRS, BP166, 38042 Grenoble Cedex 9, France*

Received 19th October 1998, Accepted 7th January 1999

Pyrochlore-type $Tl_2Mn_2O_7$ with various levels of substitution by Ru, Bi and Sb has been prepared by high-pressure synthesis at 6 GPa and 1150 °C. The ruthenium system shows a complete solid solution from $Tl_2Mn_2O_7$ to $Tl_2Ru_2O_7$. All three substituents induce an increase in cell parameter; in the case of Sb, this indicates that the substitution involves rather Sb^{5+} on Mn sites than Sb^{3+} on Tl sites. These pyrochlores start releasing thallium oxide when annealed at temperatures as low as 150 °C under 1 atm oxygen pressure; the pyrochlore phase, however, is still present at 750 °C. The partial replacement of Mn by Ru or of Tl by Bi in $Tl_2Mn_2O_7$ induces a metal–semiconductor transition, in both cases at low levels of substitution ($x<0.2$). In the ruthenium case, transport measurements in magnetic fields up to 8 T yielded a magnetoresistance $(R_0-R_H)/R_0=96\%$ in the vicinity of the metal–semiconductor transition.

Introduction

Giant magnetoresistance has been widely studied in perovskite-type manganese oxides $AMnO_3$ (A = divalent/trivalent cations).[1,2] This effect, however, has also been observed in other oxide systems: Ruddlesden–Popper phases $A_{n+1}Mn_nO_{3n+1}$ with $n=2$–3, pyrochlore-type oxides $Tl_2Mn_2O_7$,[3,4] and non-manganese perovskites such as cobaltates $ACoO_{3-x}$.[5] Among the manganese oxides, the pyrochlores are remarkable since the occurrence of giant magnetoresistance does not seem to be associated with mixed-valence manganese.[4,6]

The synthesis of Mn^{4+}-containing pyrochlores requires high-pressure syntheses, which is probably one of the reasons why this compound has been the subject of much fewer studies than perovskite-type manganites. Only one type of substitution in $Tl_2Mn_2O_7$ has been reported so far to our knowledge: the partial replacement of thallium by smaller trivalent cations such as Sc^{3+} and In^{3+}.[7,8] Such substitutions do not modify the manganese valence, but they influence magnetoresistance, which was found to be enhanced upto $(R_0-R_H)/R_H=34$ for composition $Tl_2Mn_{1.2}In_{0.8}O_7$ in a 5 T field.[7]

Numerous other cations are known to exist within the $(A^{3+})_2(B^{4+})_2O_7$ pyrochlore formula.[9] The large A site (in cubic coordination with oxygen) can accommodate rare earth cations as well as other trivalent cations such as Sc, In, Sb, Bi, while the smaller octahedral B site can contain numerous tetravalent elements ranging from titanium to silicon and tin. The aim of the present work is to explore the effect of substitutions differing from those by Sc or In: (i) isovalent substitution on the manganese sublattice, (ii) substitution on the thallium sites, but with a size or 'chemical pressure' effect applying in the opposite direction to the scandium or indium case, *i.e.* substituting a larger cation. In case (i), we chose Ru^{4+}, a very interesting cation known to induce metallicity, and even superconductivity, in several ternary oxides.[10–12] Ruthenium is also known to form a pyrochlore oxide $Tl_2Ru_2O_7$.[9] In case (ii), we chose a small cation: Sb^{3+}, and a large one: Bi^{3+}. If these cations were able to be substituted on the thallium site, they would thus allow one to extend notably the scale of chemical pressure applied on the structure: the octahedral ionic radii of trivalent Sb, Sc, In, Tl and Bi are 0.745, 0.76, 0.80, 0.88 and 1.03, respectively, according to Shannon's scale.[13]

Experimental

Powder samples of $Tl_2Mn_2O_7$, $Tl_2Mn_{2-x}Ru_xO_7$ and $Tl_{2-x}A_xMn_2O_7$ (A = Bi, Sb) were synthesized by solid-state reaction under high pressure. Stoichiometric quantities of the reactants Tl_2O_3 (Prolabo 99%), MnO_2 (Aldrich 99%), RuO_2 (Aldrich), Bi_2O_3 (Ventron 99.8%) and Sb_2O_3 (Ventron 99.7%) were mixed in an agate mortar, then sealed in a gold or platinum capsule and allowed to react at high pressure in belt-type presses. Most syntheses were carried out in a press with sample volume 42 μL, maximum pressure and temperature 8 GPa and 1200 °C. When larger volumes were sought, a bigger apparatus, labeled 'B', was used (sample volume 170 μL, maximum pressure 4 GPa). For each sample, the working temperature was maintained for 90 min, then capsules were rapidly cooled to room temperature before releasing the pressure.

Products were studied by X-ray powder-diffraction data, using a transmission diffractometer with Cu-Kα radiation and a germanium monochromator on the transmitted beam. Lattice constants were determined by a least-squares method. Products with complex powder X-ray patterns were further examined by transmission electron microscopy, using a Philips CM300 microscope operated at 300 kV and equipped with a Kevex EDS analyzer.

The stability at ambient pressure of selected samples was investigated using a Perkin-Elmer TG7 thermobalance, operated at 2 °C min^{-1} under 1 atm oxygen.

Magnetic measurements were carried out in the range 4–300 K with a SQUID magnetometer. Electrical resistivity of the samples, in the form of polycrystalline pellets, was measured using the conventional four-probe method in the temperature range 4–300 K in fields up to 8 T.

Results

1 High-pressure synthesis and solid solution formation

1.1 $Tl_2Mn_2O_7$. Several attempts allowed us to establish the optimal experimental conditions for the synthesis of $Tl_2Mn_2O_7$. Important fractions of unreacted thallium oxide remained for either too low pressure (2.5 GPa) or too low temperature (850 °C). A nearly pure $Tl_2Mn_2O_7$ phase was

obtained at 950 or 1150 °C under 6 GPa, as shown in Fig. 1, where the only lines non-indexable in the pyrochlore structure were two weak ones in the 2θ range 25–28°. These could not be attributed to any known compound in the Tl–Mn–O system, and are probably due to some unknown high-pressure phase. This point is addressed below (see section 2 below). The cell parameter of $Tl_2Mn_2O_7$ prepared in such conditions is 9.892(1) Å, in good agreement with literature values.[3,4]

All subsequent syntheses were carried out at 1050–1150 °C under 6 GPa pressure. In view of a recent study reporting widely different transport properties in $Tl_2Ru_2O_7$ prepared under pressure with or without the presence of an oxidizer,[14] an additional synthesis run was carried out in the same conditions, with the addition of *ca.* 10 wt.% potassium chlorate. X-Ray diffraction showed that it contained a large fraction of unreacted thallium oxide, and that the cell parameter of the pyrochlore phase formed was not significantly different from that obtained without oxidizer [$a=9.891(8)$ Å].

1.2 $Tl_2Mn_{2-x}Ru_xO_7$ system. High-pressure synthesis with mixtures of nominal composition $Tl_2Mn_{2-x}Ru_xO_7$ yielded similar X-ray patterns, with a shift of the observed reflections towards low angles indicating a larger unit cell (see Fig. 1, top). The substituted sample reflections have larger linewidths, which may indicate inhomogeneities in ruthenium distribution. This can also be due to differences in synthesis conditions: the ruthenium series was prepared using the larger B press, operated at 4 GPa instead of 6 GPa for unsubstituted $Tl_2Mn_2O_7$. Refined cell parameters are shown in Fig. 2 as a function of ruthenium content. The monotonous increase in cell constant, as well as the absence of additional lines, shows that a continuous solid solution exists between the two pyrochlores phases $Tl_2Mn_2O_7$ and $Tl_2Ru_2O_7$. The cell parameter variation is in agreement with the difference in octahedral ionic radius between Mn^{4+} (0.53 Å) and Ru^{4+} (0.62 Å).

1.3 Bismuth substitution. Samples of $Tl_{2-x}Bi_xMn_2O_7$ were first prepared using platinum crucibles. Whereas no significant difference was observed for Ru-substituted samples between Au and Pt containers, the use of platinum crucibles with bismuth-containing mixtures systematically yielded X-ray patterns with all pyrochlore lines split into two components (particularly visible at high angles in Fig. 3, bottom), as if two pyrochlore-type phases with slightly different cell parameters had been formed.

EDS analysis in the electron microscope showed indeed the presence of two phases with widely differing compositions: a thallium platinate with Tl:Pt ratio ≈ 1.0, and a manganese-rich phase with a composition close to $TlMn_3O_x$. The former corresponds to $Tl_2Pt_2O_7$, a known pyrochlore-type oxide with a slightly larger cell parameter than manganese pyrochlores. This phase was previously found to form under high pressure from the interaction between thallium oxide and platinum crucibles.[15]

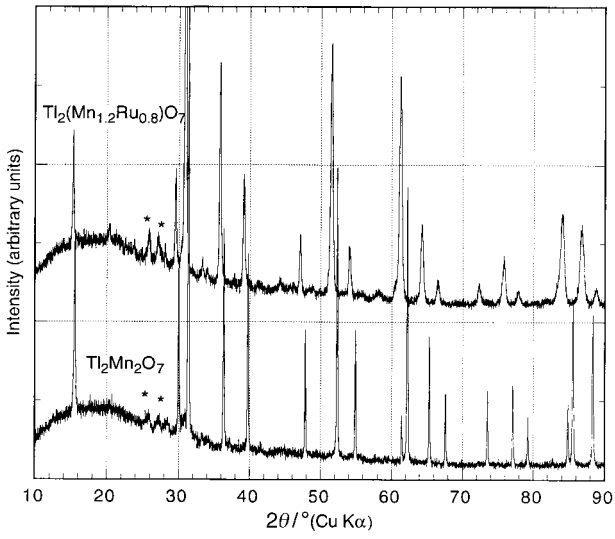

Fig. 1 X-Ray powder diagrams of $Tl_2Mn_2O_7$ (bottom) and $Tl_2Mn_{1.2}Ru_{0.8}O_7$ (top) prepared at 1150 °C and 6 GPa. Impurity lines are indicated by asterisks.

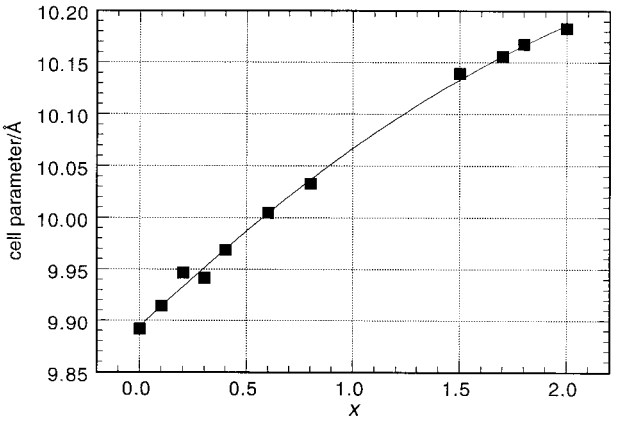

Fig. 2 Evolution of the $Tl_2Mn_{2-x}Ru_xO_7$ cubic cell parameter as a function of x.

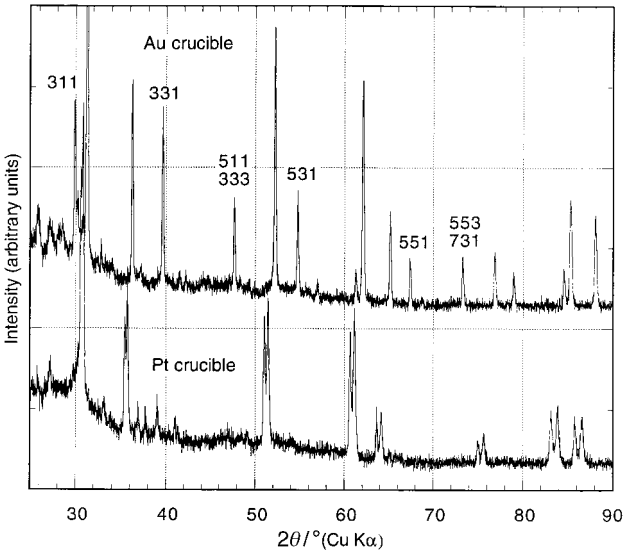

Fig. 3 X-Ray powder diagrams of $Tl_{1.7}Bi_{0.3}Mn_2O_7$ prepared in a platinum (bottom) and in a gold (top) container. Odd *hkl* indices shown are those of pyrochlore reflections which are not observed in the bottom pattern (see text).

Electron diffraction confirmed that the new Mn-rich phase is cubic. It also exhibits diffuse lines, indicating a more complex structure probably involving cation ordering. Its stoichiometry can be accounted for by the occupation of A sites by Mn^{2+} cations, as in the known $(LnMn^{2+})(MnSb)O_7$ series.[9] The formation of a Mn^{2+}-containing phase is all the more plausible that platinum acts as a reducing agent in this process. The redox reaction with platinum could thus be written:

$$3\ \text{`}Tl_2Mn_2O_7\text{'} + 4\ Pt \rightarrow 2\ (TlMn^{2+})(Mn^{4+})_2O_{6.5} + 2\ Tl_2Pt_2O_7$$

yielding an oxygen-deficient pyrochlore $A_2B_2O_{6.5}\square_{0.5}$.

Pyrochlore oxides are notorious for easily accepting oxygen vacancies on the O2 (8b) site.[9] Several examples are known with 0.5 oxygen vacancies;[16,17] this stoichiometry gives rise to a supercell resulting from vacancy ordering. Vacancy ordering and/or short-order cation ordering on the A sites could be the cause of the diffuse lines observed here in electron diffraction.

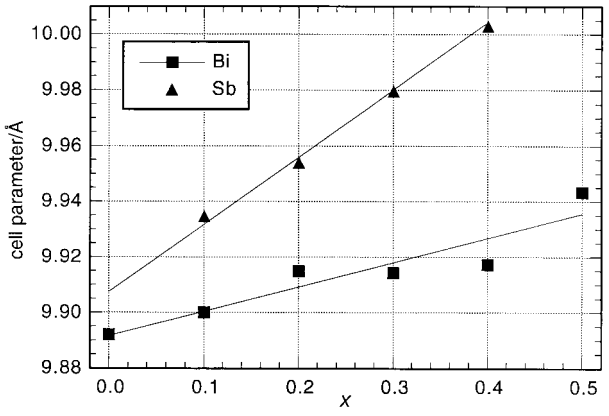

Fig. 4 Evolution of the cubic cell parameter of $Tl_{2-x}A'_xMn_2O_7$ (A′= Bi, Sb) as a function of x.

The X-ray patterns of both the Mn-rich phase and $Tl_2Pt_2O_7$ are also remarkable because of additional extinctions, which were already noted in $Tl_2Pt_2O_7$.[15] In the pyrochlore structure, the main contribution to the intensity of all-odd (*hkl*) reflections is the difference in scattering power between A- and B-site cations.[16] This difference is related to the difference in atomic number ΔZ, which is equal to 56, 28 (average) and 3 in $Tl_2Mn_2O_7$, $TlMn_3O_{6.5}$ and $Tl_2Pt_2O_7$, respectively, explaining the observed extinctions.

When the synthesis is carried out in gold, the parasitic reaction with the container is suppressed and a unique pyrochlore phase is obtained (see Fig. 3, top). The all-odd (*hkl*) extinctions are not observed (compare Fig. 3, top and bottom), in agreement with the stoichiometry. The evolution of the cell parameter as a function of bismuth content (Fig. 4) shows the presence of a solid solution at least up to $x(\mathrm{Bi})=0.5$. As in the Ru/Mn substitution, the replacement of thallium by larger bismuth induces a monotonous increase in cell parameter. However, a comparison of the y-scales in Fig. 2 and 4 shows that the influence of Bi substitution on the A sites is quantitatively much smaller than that of Ru on the B sites, in spite of a similar ionic radius difference between the Ru/Mn and Bi/Tl pairs (+18%). This different behaviour could be ascribed (1) to the larger polarizability of Bi^{3+}, which carries exactly twice as many electrons as Ru^{4+}, (2) to the larger rigidity of the octahedral sites compared to the large, cubic A sites in the pyrochlore structure.

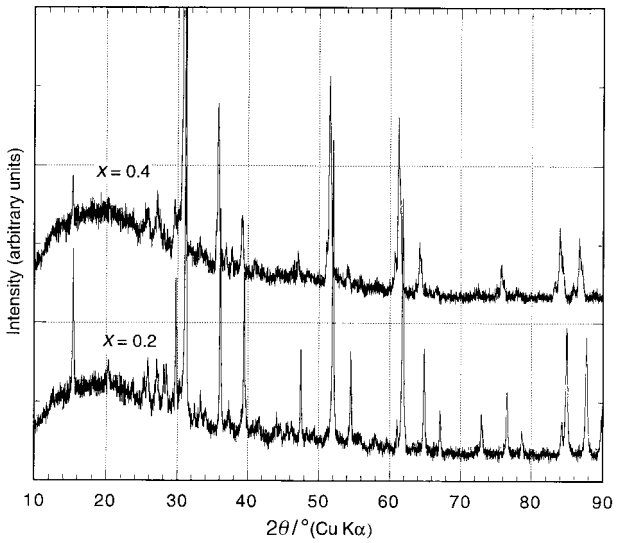

Fig. 5 X-Ray powder diagrams of samples of nominal composition $Tl_{2-x}Sb_xMn_2O_7$ with $x=0.2$ and 0.4.

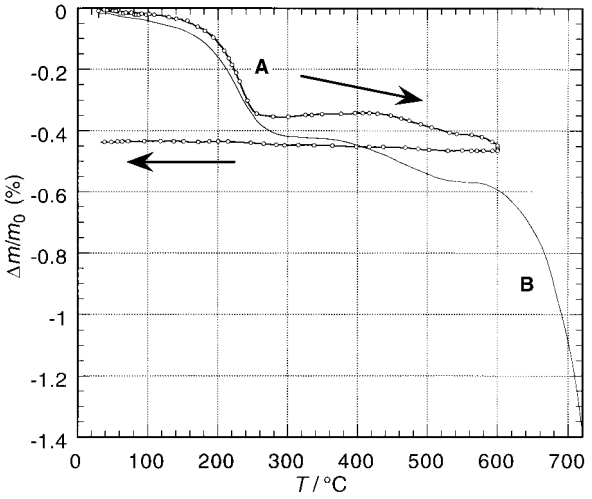

Fig. 6 Thermogravimetric behaviour of $Tl_2Mn_{2-x}Ru_xO_7$ in 1 atm oxygen. Maximum temperatures 600 °C (A), 750 °C (B).

1.4 Antimony substitution. Samples of nominal composition $Tl_{2-x}Sb_xMn_2O_7$ ($x\leqslant 0.4$) were submitted to a similar high-pressure, high-temperature treatment in gold crucibles. X-Ray diffraction patterns show the occurrence of a single-phase pyrochlore-type phase for all x values (see Fig. 5). However, in spite of the fact that Sb^{3+} has a smaller ionic radius than Tl^{3+}, the cell parameter *increases* with increasing Sb content (see Fig. 4 and 5). This result suggests a different charge distribution, namely the coexistence Sb^{5+}–Mn^{2+} rather than Sb^{3+}–Mn^{4+}. The smaller Sb^{5+} cation occupies B sites, as in the known $RE(CrSb)O_7$ series (RE = rare earth),[9] while manganese migrates partially to the A sites as Mn^{2+}, giving the formula $(Tl_{2-x}[Mn^{2+}]_x)([Mn^{4+}]_{2-x}[Sb^{5+}]_x)O_7$. The evolution of the cell parameter is then determined by the B sites occupation, where Sb^{5+} is indeed larger than Mn^{4+} (octahedral ionic radii 0.60 and 0.53, respectively). The cell parameter variation with antimony content is almost linear up to $x=0.4$ (see Fig. 4). This model is also consistent with the standard redox potentials of the MnO_2/Mn^{4+} and

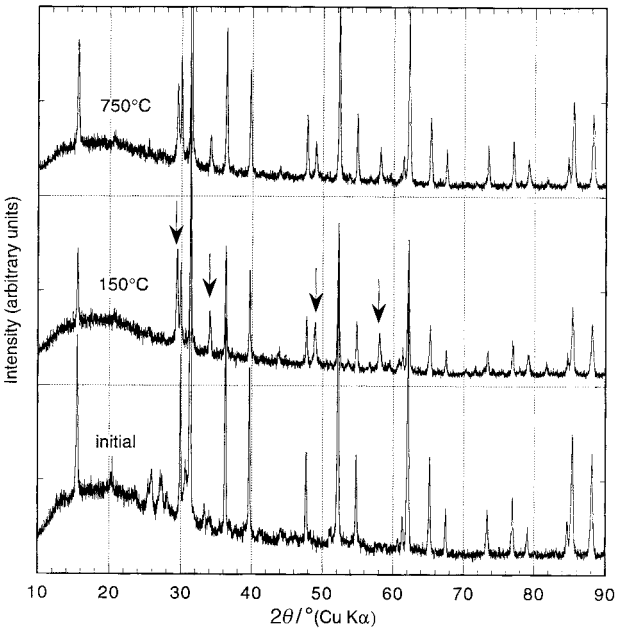

Fig. 7 X-Ray powder diagrams of $Tl_2Mn_{1.9}Ru_{0.1}O_7$ after annealing in 1 atm oxygen at 150 °C (middle) and 750 °C (top). Note the disappearance of the extra lines at 26–29° and the prominent Tl_2O_3 lines in annealed samples (indicated by arrows).

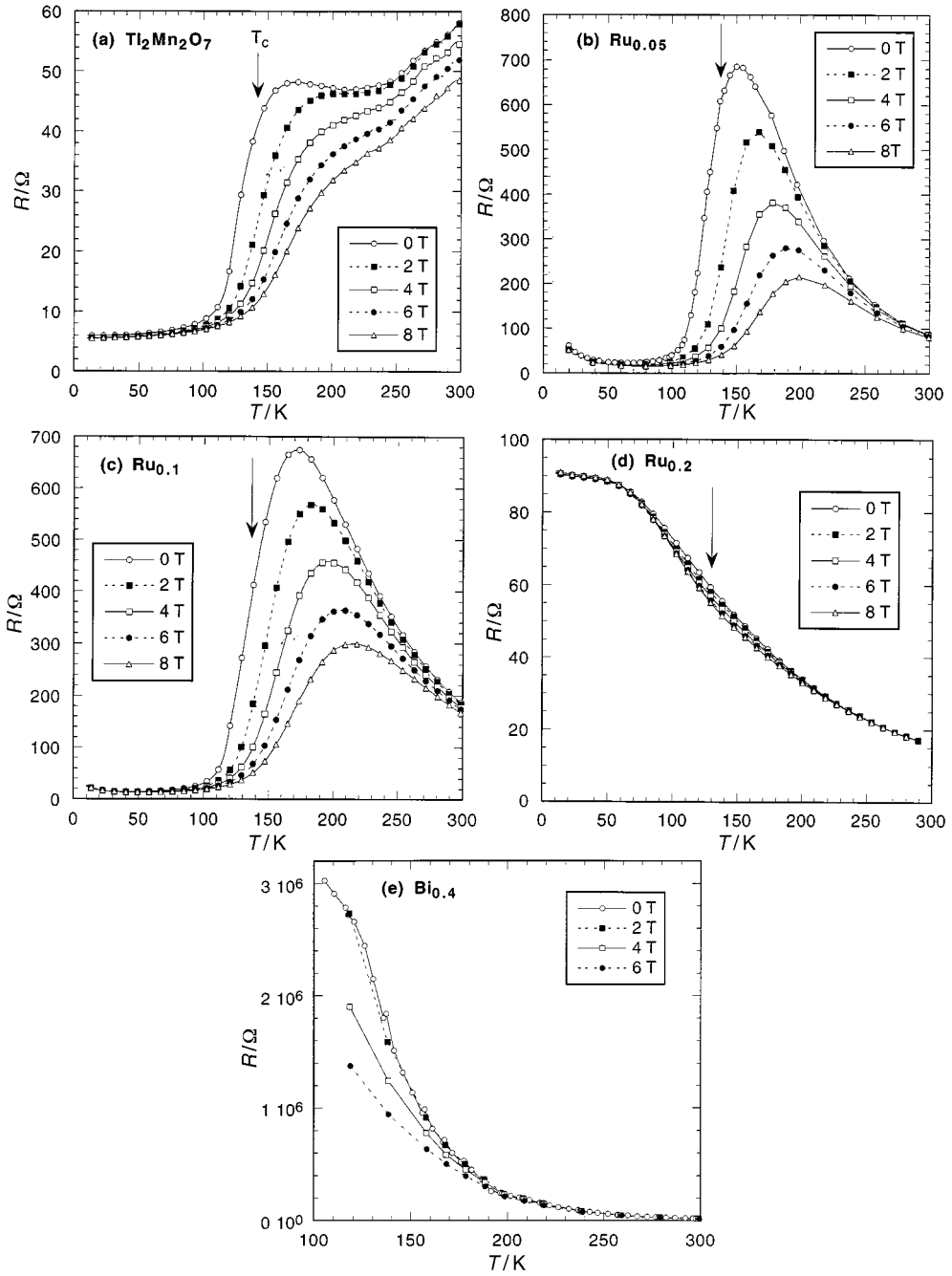

Fig. 8 Variation of the electrical resistance with temperature and magnetic field in the $Tl_2Mn_{2-x}Ru_xO_7$ and $Tl_{2-x}Bi_xMn_2O_7$ systems: (a) $Tl_2Mn_2O_7$, (b) $x_{Ru}=0.05$, (c) $x_{Ru}=0.1$, (d) $x_{Ru}=0.2$, (e) $x_{Bi}=0.4$. Arrows indicate the Curie temperatures.[22]

Sb_2O_5/Sb_2O_3 couples (1.21 and 0.69 V, respectively),[18] and the existence of stable Mn(II) antimoniates(V), such as $MnSb_2O_6$ or $Mn_2Sb_2O_7$.[19]

2 Thermal stability under ambient pressure

Selected ruthenium-substituted samples were investigated by thermogravimetry under 1 atm oxygen pressure. The resulting curves (Fig. 6) show a slight mass loss A at $T<250\,^{\circ}C$, a plateau up to *ca.* 600 °C, and finally a more important mass drop B at higher temperatures. These variations are irreversible in oxygen.

The X-ray patterns of samples after thermogravimetric treatment (Fig. 7) show that mass loss A is connected with two structural changes: (i) the disappearance of the small unknown lines at $2\theta=25$–28°, (ii) the appearance of Tl_2O_3 lines, indicating partial decomposition of the pyrochlore oxide. These effects were observed after annealings at temperatures as low as 150 °C in 1 atm oxygen (see Fig. 7).

Mass loss B is due to further thallium losses in the form of sublimating thallous oxide. This compound is notorious for its high volatility, and is the stable form of thallium oxide at high temperature. Because of these thallium losses, thermogravimetry does not allow one to detect whether oxygen vacancies can be introduced in $Tl_2Mn_2O_7$ by temperature annealings at ambient pressure.

3 Transport properties

Fig. 8 shows the electrical resistance as a function of temperature and magnetic field in the $Tl_2Mn_{2-x}Ru_xO_7$ system. A wide hump occurs just above the Curie temperature (marked by arrows in Fig. 8(a)–(d)). Dramatic changes in the resistance variation with respect to pure $Tl_2Mn_2O_7$ are observed for substitution levels as low as $x=0.05$: (i) the hump around 150–160 K is considerably enhanced, (ii) the high-temperature part now shows a semiconducting variation. This metal–insulator transition induces a large magnetoresistance

$(R_0-R_H)/R_0$ (up to 95% at 160 K). For $x=0.2$, the behaviour is that of a semiconductor in the whole temperature range [Fig. 8(d)]. The substitution by bismuth also destroys the metallic conductivity at low substitution fractions [see Fig. 8(e)]. To our knowledge, such an effect was not reported previously.

In order to better characterize the resistivity changes on substitution in $Tl_2Mn_2O_7$, we compared the fits of resistivity in the paramagnetic range to (i) an activated regime:

$$\ln(R)=A+\exp(E_a/kT)$$

(ii) a variable-range hopping regime following Mott's law:[20]

$$\ln(R)=A+(T_0/T)^{1/4}$$

For $Tl_2Mn_{1.95}Ru_{0.05}O_7$, the activation law would give an activation energy equivalent to $(E_a/k)=1033$ K at zero field. However the fit is better using a $(T_0/T)^{1/4}$ dependence [see Fig. 9(a)]. In this case, the Mott parameter $T_0{}^{1/4}$, which is proportional to the localisation energy,[21] is found to decrease with the applied field, from 62.8 $K^{1/4}$ in zero field to 50.0 $K^{1/4}$ under 8 T. The same trend is observed for higher ruthenium contents (in $Tl_2Mn_{1.9}Ru_{0.1}O_7$, $T_0{}^{1/4}=51.0$ and 36.7 $K^{1/4}$ under 0 and 8 T, respectively).

A second localisation regime is observed below 40 K for 0.05 Ru substitution [see Fig. 8(b)], and is clearly valid on a much larger temperature range than an activation law. It gives $T_0{}^{1/4}\approx 6.5$ $K^{1/4}$, almost field-independent. This may be an indication of localisation, which is strongly dependent on magnetic disorder, but much less on atomic disorder.

Fig. 10 shows the evolution of the maximum magnetoresistance MR_{max} as a function of ruthenium content in the $Tl_2Mn_{2-x}Ru_xO_7$ system. MR_{max} is highest for $x=0.05$, where it reaches *ca.* 94% (or 1380% with respect to R_H). In the case of indium substitution, the maximum magnetoresistance was tentatively correlated with the presence of a miscibility gap in the $Tl_2Mn_{2-x}In_xO_7$ solid solution.[7] No such effect is observed here. As also shown in Fig. 10, the temperature of MR_{max} decreases with increasing ruthenium content, following the evolution of the Curie temperature T_c, but remaining systematically slightly higher than T_c (see arrows in Fig. 8). The magnetic behaviour of the $Tl_2Mn_{2-x}Ru_xO_7$ system is discussed in more detail elsewhere.[22,23]

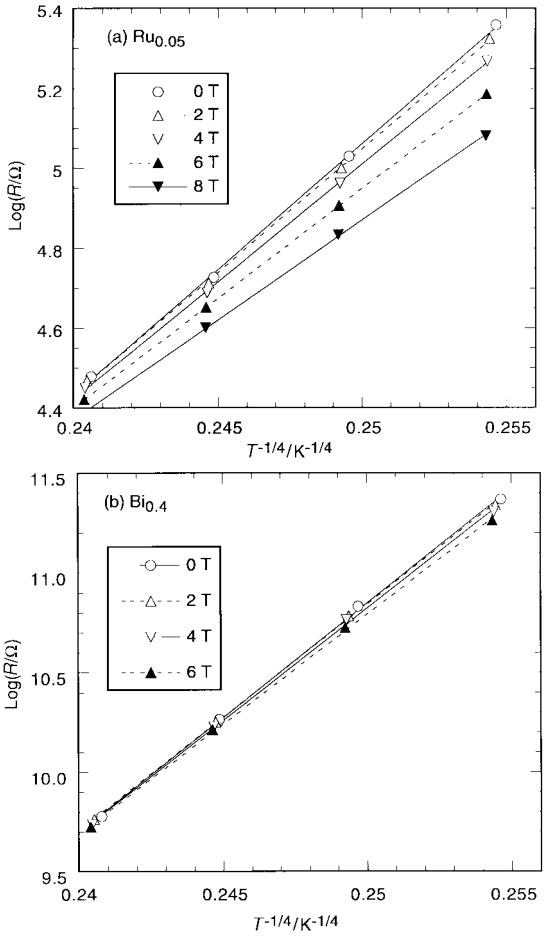

Fig. 9 Fits of the resistivity to Mott's law in the paramagnetic range. (a) $Tl_2Mn_{1.95}Ru_{0.05}O_7$, (b) $Tl_2Mn_{1.6}Bi_{0.4}O_7$.

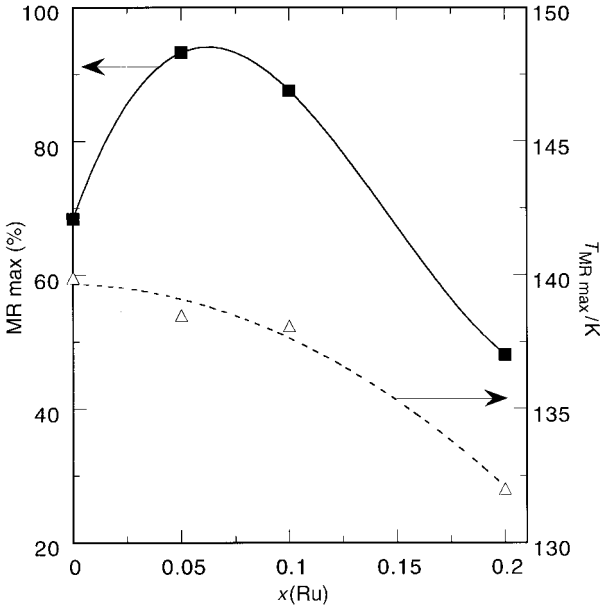

Fig. 10 Evolution of maximum magnetoresistance $MR_{max}=(R_0-R_H)/R_0$ under 8 T (squares) and of the temperature of MR_{max} (triangles) as a function of Ru content x. The lines are guides to the eye.

In the case of bismuth-substituted $Tl_2Mn_2O_7$, the activation law is only followed in a narrow range below 300 K, where it gives $(E_a/k)\approx 1880$ K, much higher than in the ruthenium case. The data again fit better Mott's law in the paramagnetic range, giving $T_0{}^{1/4}=112.4\pm 2.4$ $K^{1/4}$, almost field-independent [see Fig. 9(b)]. The higher resistivity and $T_0{}^{1/4}$ variation may be a consequence of the higher scattering potential of bismuth, which carries two additional 6s electrons.

Discussion

Giant magnetoresistance has been observed mainly in manganese oxides with perovskite structure.[1,2] A comparison between these and pyrochlore systems shows two important differences: (i) the Mn–O–Mn bond angles are *ca.* 180° in perovskites, but 133–134° in $Tl_2Mn_2O_7$,[3,4] which modifies considerably the magnetic interaction mechanism, (ii) whereas the temperature and magnitude of magnetoresistance strongly depend on the manganese valence v(Mn) in perovskites, where v(Mn) can be adjusted by appropriate alkaline-earth cation substitution for lanthanum, no evidence of mixed Mn^{3+}/Mn^{4+} valence has been found in pyrochlore manganates,[4,6] and the carrier density is much smaller. Instead of the classical dependence of transport properties and magnetoresistance on charge doping, the physical properties are found to vary considerably with substitution by *isovalent* cations such as In, Sc or Bi for Tl, or Ru for Mn. These experimental facts may indicate that magnetic and transport properties are very sensitive to minor changes in metal–oxygen bonding distances and angles. In addition, bismuth, thallium and ruthenium all can give rise to mixed-valence just as manganese. An overlapping of the Tl 6s and Mn 3d bands has been proposed as a cause of internal mixed valence and source of charge carriers.[4]

The observed $R(T)$ laws seem to show the importance of localisation processes giving rise to spin polarons.[23] Localisation at low temperature is favoured by atomic disorder, hence the increase in semiconducting character with cation substitution. Increasing the internal field or the applied magnetic field reduces carrier localisation by shifting the Fermi energy towards the mobility edge for up and down spin subbands, giving rise to the magnetoresistance effect.

Finally, the possibility of a small oxygen non-stoichiometry in pyrochlore-type manganates cannot be ruled out.[4,24] Unfortunately, this effect is difficult to ascertain accurately in compounds which are available in small quantities only because of the high-pressure synthesis limitations, and which release thallium oxide when heated, precluding any measurement of oxygen content variation by thermogravimetry. Additional experiments, especially by X-ray absorption, are planned to study in more detail the manganese valence issue in substituted pyrochlore manganates.

Conclusions

A number of substitutions were carried out in $Tl_2Mn_2O_7$. A complete solid solution was found on the B site between manganese and ruthenium. Bismuth can be partially substituted for thallium on the A sites, while antimony enters the B sites following an internal oxido–reduction reaction $Sb^{3+}+Mn^{4+}\rightarrow Sb^{5+}+Mn^{2+}$. A new mixed-valence Mn-rich phase $(TlMn^{2+})Mn_2O_x$ was obtained when thallium was partially trapped by a side-reaction with the platinum container. The metallic conductivity in $Tl_2Mn_2O_7$ is broken by small amounts of doping on the thallium site (Bi case) as well as on the Mn one (Ru case). In the latter, a large magnetoresistance effect is observed in the range 130–150 K and is maximum for compositions close to the metal–semiconductor transition. The enhancement of magnetoresistance by isovalent cation doping, as well as the negligible influence of synthesis in the presence of an oxidizer point to a mechanism differing significantly from that in the perovskite-type manganates.

Acknowledgements

The authors wish to thank J. C. Joubert (LMGP Grenoble) and M. Pernet for fruitful discussions.

References

1 A. P. Ramirez, *J. Phys. Condens. Matter*, 1997, **9**, 8171.
2 C. N. R. Rao and A. K. Cheetham, *Adv. Mater.*, 1997, **9**, 1009.
3 Y. Shimakawa, Y. Kubo and T. Manako, *Nature*, 1996, **379**, 53; Y. Shimakawa, Y. Kubo, T. Manako, Y. V. Sushko, D. N. Argyriou and J. D. Jorgensen, *Phys. Rev. B*, 1997, **55**, 6399.
4 M. A. Subramanian, B. H. Toby, A. P. Ramirez, W. J. Marshall, A. W. Sleight and G. H. Kwei, *Science*, 1996, **273**, 81.
5 C. Martin, A. Maignan, D. Pelloquin, N. Nguyen and B. Raveau, *Appl. Phys. Lett.*, 1997, **71**, 1421.
6 H. D. Rosenfeld and M. A. Subramanian, *J. Solid State Chem.*, 1996, **125**, 278.
7 S. W. Cheong, H. Y. Hwang, B. Batlogg and L. W. Rupp, *Solid State Commun.*, 1996, **98**, 163.
8 A. P. Ramirez and M. A. Subramanian, *Science*, 1996, **273**, 81.
9 M. A. Subramanian and A. W. Sleight, in *Handbook on the Physics and Chemistry of Rare Earths*, ed. K. A. Gschneider and L. Eyring, Elsevier, Amsterdam, 1993, **16**, 225.
10 Y. Maeno, H. Hashimoto, K. Yoshida, S. Nishizaki, T. Fujita, J. G. Bednorz and F. Lichtenberg, *Nature*, 1994, **372**, 532.
11 H. Kobayashi, R. Kanno, Y. Kawamoto, T. Kamiyama, F. Izumi and A. W. Sleight, *J. Solid State Chem.*, 1995, **114**, 15.
12 G. Cao, S. C. McCall, J. E. Crow and R. P. Guertin, *Phys. Rev. B*, 1997, **56**, 5387.
13 R. D. Shannon, *Acta Crystallogr., Sect. A*, 1976, **32**, 751.
14 T. Takeda, M. Nagata, H. Kobayashi, R. Kanno, Y. Kawamoto, M. Takano, F. Izumi and A. W. Sleight, *J. Solid State Chem.*, 1998, **140**, 182.
15 H. R. Hoekstra and S. Siegel, *Inorg. Chem.*, 1968, **7**, 141.
16 R. A. Beyerlein, H. S. Horowitz, J. M. Longo, M. E. Leonowicz, J. D. Jorgensen and F. J. Rotella, *J. Solid State Chem.*, 1984, **51**, 253.
17 B. J. Kennedy, *J. Solid State Chem.*, 1996, **123**, 14.
18 *Handbook of Chemistry and Physics*, ed. D. R. Lide, 76th edn., CRC Press, Boca Raton, FL, 1995.
19 JCPDS Files No. 38-1351 and 39-0980.
20 N. F. Mott, *Metal–Insulator Transitions*, Taylor & Francis, London, 2nd edn., 1990.
21 T. G. Castner, in *Hopping Transport in Solids*, ed. M. Pollak and B. Sklovskii, North-Holland, Amsterdam 1991, p. 9.
22 R. Senis, B. Martinez, X. Obradors, W. Cheikh-Rouhou, C. Chaillout, M. Pernet and P. Strobel, *J. Appl. Phys.*, 1999, **74**, in press.
23 B. Martinez, R. Senis, J. Fontcuberta, X. Obradors, W. Cheikh-Rouhou, P. Strobel, C. Chaillout and M. Pernet, to be published.
24 N. P. Raju, J. E. Greedan and M. A. Subramanian, *Phys. Rev. B*, 1994, **49**, 1086.

Paper 8/08086K